2017 International Conference on Rehabilitation Robotics (ICORR)
QEII Centre, London, UK, July 17-20, 2017.

Estimating Anatomical Wrist Joint Motion with a Robotic Exoskeleton

Chad G. Rose† *Student Member, IEEE*, Claudia K. Kann† *Student Member, IEEE*,
Ashish D. Deshpande‡ *Senior Member, IEEE*, and Marcia K. O'Malley† *Senior Member, IEEE*

***Abstract*— Robotic exoskeletons can provide the high intensity, long duration targeted therapeutic interventions required for regaining motor function lost as a result of neurological injury. Quantitative measurements by exoskeletons have been proposed as measures of rehabilitative outcomes. Exoskeletons, in contrast to end effector designs, have the potential to provide a direct mapping between human and robot joints. This mapping rests on the assumption that anatomical axes and robot axes are aligned well, and that movement within the exoskeleton is negligible. These assumptions hold well for simple one degree-of-freedom joints, but may not be valid for multi-articular joints with unique musculoskeletal properties such as the wrist. This paper presents an experiment comparing robot joint kinematic measurements from an exoskeleton to anatomical joint angles measured with a motion capture system. Joint-space position measurements and task-space smoothness metrics were compared between the two measurement modalities. The experimental results quantify the error between joint-level position measurements, and show that exoskeleton kinematic measurements preserve smoothness characteristics found in anatomical measures of wrist movements.**

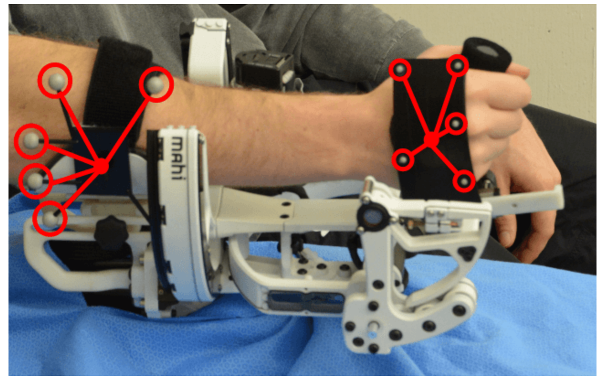

Fig. 1. The OpenWrist [12], part of the integrated hand and wrist exoskeleton READAPT, evaluated as a measurement device via movement smoothness analysis. Rigid bodies defined by passive motion capture markers used to measure relative wrist angles are highlighted in red.

I. INTRODUCTION

Regaining lost motor function after neuromuscular conditions such as stroke or spinal cord injury requires long duration, high intensity therapy sessions involving high levels of patient engagement [1]. To retrain the ability to perform activities of daily living (ADL), exoskeletons targeting the upper extremity have been developed [2], and have been verified in clinical studies [3]. In particular, the wrist is garnering attention due to its role in dexterous manipulation. Rehabilitation robots for the wrist have been proposed, such as Pehlivan, et. al [4] and Masia, et. al [5]. The READAPT [6] combines a wrist exoskeleton with a hand exoskeleton. Often these devices are used both for delivering therapy and for assessing rehabilitation outcomes.

Robots offer capabilities for measurement modalities typically not available to clinicians, who often rely solely on functional assessments such as GRASSP [7] or Box and Blocks [8]. Tyryshkin et. al [9] propose objective measurements created from tracking hand position in Cartesian space that correlate with established measures, and provide greater detail in assessing motor function post stroke than traditional methods. Exoskeleton designs such as the READAPT have similar capability at measuring motor function in task spaces, as well as the potential to access individual joint level measurements. The mapping between human joints and robot joints enables analyses of joint-level movement characteristics not available in either traditional clinical measures or task-space measurements [10], [11]. For practical considerations, these benefits are maximized when the same device is used for training and measurement.

A few assumptions are made in these joint-level measures, namely that using the measurement device doesn't affect the measurand, and measurements of robot joints are sufficient for inferring human joint angles. Previous studies have shown how measurement via the READAPT affected the measurand for coordinated movements of the hand and wrist [6]. Key assumptions about device transparency were tested, namely that 'low' inertia and static friction properties were sufficient to ensure accurate measurement, and comparisons between passive backdriving and active zero-impedance modes were made. While this preliminary study examined the impact of a wearable device on movement, it did not verify that the measurements of robotic joint angles correspond to human joint angles. Separately, the accuracy of torque and position measurements of the hand exoskeleton module of the READAPT have been presented [13], validating the hand exoskeleton's measurements. However, the wrist portion of the device [12] has not been examined in detail. In particular, the impact of ergonomic considerations to prevent kinematic overconstraint on measurement need to be evaluated.

Devices rely on a variety of features, from passive degrees of freedom [4] to anatomically designed wrist mechanisms [14], to align exoskeleton joints to the complex rotations in the wrist. However, preventing kinematic overconstraint is not enough to ensure that robotic joint measurements are accurate reflections of human joint measurements, in particular when unmeasured movement is part of the design.

†Mechatronics and Haptic Interfaces Lab, Mechanical Engineering Department, Rice University, Houston, TX 77005 USA. cgr2@rice.edu
‡ReNeu Robotics Lab, Department of Mechanical Engineering, University of Texas at Austin, Austin, TX, USA.

To this end, we present a preliminary experimental validation of the OpenWrist [12], the READAPT wrist module, as a measurement tool for wrist movements of able-bodied individuals. Section II describes the experimental validation methods, and Section III presents the findings of the experiment. Section III-A compares the measurements of the device in terms of position, discussing the limitations of both the experimental methods, exoskeleton device, and arbitrary wrist axis conventions. Section III-B presents two movement smoothness metrics calculated with robotic and anatomical joint measurements, putting the results of the experiment in the context of how these devices are often used.

II. EXPERIMENTAL METHODS

We are interested in investigating the suitability of our exoskeleton as a rehabilitation assessment device. To this end, we recorded movements with a motion capture system and the exoskeleton's integrated sensors while subjects completed a multi-DOF pointing task. We selected isolated and combined wrist flexion/extension and radial/ulnar deviation movements for their unique physcial and movement properties [15]. A task similar to prior work [15] and therapeutic tasks [16] allows us to investigate the effect of anatomical and robotic joint misalignment and movement within the robot on measurements of complex joints such as the wrist.

A. Task Description

The task required pointing movements to nine targets, one at a constant position near neutral, and eight targets displayed on a circle, shown in Fig. 2. Subjects were instructed to reach the targets at a speed suggested by the closing of a gate around the target, shown in Fig. 2b and Fig. 2c. Subjects reached each target five times in a practice session then 15 times in a psuedo-random order for two speed conditions, 'slow' and 'fast', which suggested 0.6 and 0.4 seconds respectively, to complete the task. To simplify segmentation based on velocity thresholds, subjects were required to wait on all targets for one second.

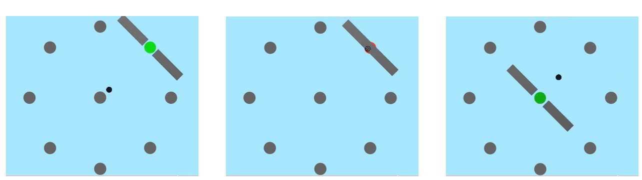

(a) Task start (b) Outbound reached (c) Return

Fig. 2. Subjects begin at the center target, then a goal target is highlighted and blocks appear, closing at a rate that suggest the time allowed for the movement. Then, after reaching the outer target, subjects return to the center.

While the visualization shown to the user was circular, the mapping between each target position and the required wrist angles was chosen to reflect a constant portion of the ROM, and not a constant angular distance, as shown in Fig. 3. The target locations were selected by taking the average wrist ROM defined by Crisco, et. al, [17], reducing it by 40%, and spreading targets every 45° around the edge of the reduced workspace. The cursor moved in a linearly scaled fashion with radial/ulnar deviation corresponding to up/down, and flexion/extension corresponding to left/right, respectively, as measured by the motion capture system.

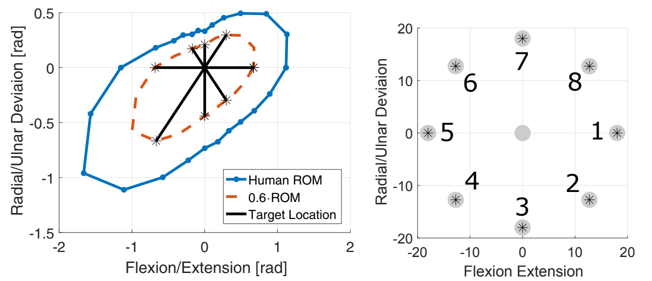

(a) Range of Motion Scaling (b) Visualization

Fig. 3. Target positions were created by scaling the workspace proposed by Crisco et. al [17] by 40%. Targets were placed around the work space at 45° intervals, marked by asterisks. The visualization displayed a circular workspace, but the distance from center to the desired target was scaled to the red ellipse in (a). The units in (b) are positions in the visualization.

B. Subjects

Nine subjects, two female, seven male, ages 20-28 were tested in compliance with the Rice University Institutional Review Board. All subjects were right hand dominant, with no known wrist impairments or history of injury.

C. Kinematic Joint Angle Measurement

When acting as a measurement tool, the OpenWrist, shown in Fig. 1, is unpowered, backdriven, and measurements are taken from the 500 count Avago HEDL-5540 quadrature encoders at each robotic joint. The sensor resolution of this device is on the order of hundredths of a degree, similar to previously presented devices [4]. Encoder velocity is obtained with a Q8-USB DAQ from Quanser.

D. Anatomical Joint Angle Measurement

Human wrist angles were measured with a motion camera system. Six Optitrack Flex V100R2 100 FPS cameras, 3 mm and 11 mm passive reflective markers for the hand and forearm (shown in Fig. 1), respectively, were used in conjuction with QuaRC and Simulink in Windows to measure the relative joint angles in soft real time during the pointing tasks. Markers were used to create rigid bodies, whose orientation relative to the motion capture world frame were recorded by QuaRC and Simulink. An algorithm, proposed by Biryukova et. al [18] was used to determine an estimate of the anatomical wrist rotations. This implementation is more similar to magnetic motion tracking methods than most implementations of optical motion capture of wrist movements in that marker placement is not a function of anatomical landscape [19], removing requirements about the location and accuracy of optical marker placement. However, concerns about movement of markers on the skin is still present, which the use of physical rigid bodies, highlighted in red in Fig. 1 sought to minimize.

The algorithm is defined in detail by Biryukova et. al [18], but is repeated here in brief to clarify the results of partial differentiation and the selection of the eigenvalue.

The algorithm uses the orientation of two rigid bodies, the forearm and hand, to the world frame and estimates axes of rotation based on single DOF calibration movements. The orientation of the axis is obtained by minimizing the integral

$$\Delta\omega = \frac{1}{t}\int_0^t (R_1\omega_1 - R_2\omega_2)^2 dt \qquad (1)$$

where ω_1 and ω_2 are the orientations of the axes with respect to the hand and forearm, R_1, R_2 are the orientation of the rigid bodies with respect to the world frame, and t is the duration. The partial derivative of (1) with respect to ω_1 and ω_2 gives a linear system of equations

$$\begin{bmatrix} I & -\int_0^t R_1^T R_2 dt \\ -\int_0^t (R_2^T R_1 dt & I \end{bmatrix} \begin{bmatrix} \omega_1 \\ \omega_2 \end{bmatrix} = 0 \qquad (2)$$

where the integrals were determined via `trapz` in MATLAB. The eigenvalue of the matrix given in (2) where the smallest magnitude corresponds to the axis orientation which minimizes the originally proposed integral in (1). Repeating the process for another movement results in the other axis orientation. Taking the cross product of the two resulting axes creates a third orthogonal axis, which for the purposes of this study was not considered to correspond to pronation/supination, since no calibration of that DOF was made. Crossing this third axis with an anatomical axis creates an orthogonal set of anatomically inspired axes, which was used to determine wrist angles, as clarified in Fig 4.

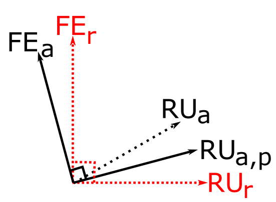

Fig. 4. Simplified 2D schematic illustrating the 3D calibration and defintion of the anatomical axes, with 'r' subscripts representing robot axes, 'a' subscripts representing calibrated anatomical axes, and 'a,p' representing the change made to the RU axis to impose orthogonality.

The sample calibration movements in Fig. 5 show the wrist angles about the calibrated axes along with the measurements of the robot joint encoders. The difference between the motion capture and the encoder measurements are likely a function of both the anatomically calibrated axes' misalignment with the robot joints, and the limitations of assuming a constant axis position and orientation to represent anatomical joint axes. In the next section, we quantify these differences and evaluate the impact on robotic metrics of movement quality derived from the joint angle measurements.

E. Data Analysis

Anatomical joint measurements were filtered and differentiated using a third order Savitzky-Golay filter with a 21-sample (200ms) window [20]. Inbound and outbound movements were segmented in two ways. First, kinematic and anatomical trajectories were segmented independently, at the point where the velocity profile first exceeded, then

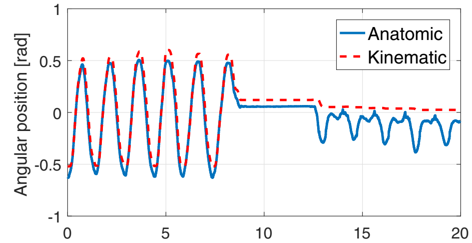

(a) Radial/ulnar deviation calibration movement

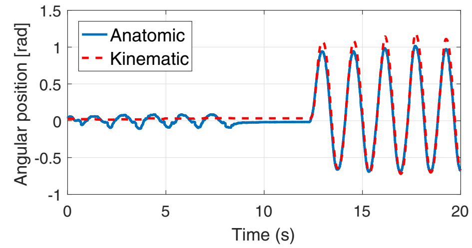

(b) Flexion/extension calibration movement

Fig. 5. Single DOF calibration movements were used to determine anatomical axes, plotted against the robot kinematic measured during the same movements. Positive rotations were defined as wrist flexion and radial deviation. The error in these joint level trajectories is largely a result of anatomical and kinematic misalignment.

fell below 2% of the movement's maximum velocity [21], without knowledge of the other measurement modality. This selected threshold compares with other implementations of 1% [22] and 5% [15] thresholds. Then, to reduce the effect the variations introduced by separately segmenting each movement, the motion capture and joint encoder movements were segmented at the same point, using the velocity threshold crossing information from both movements, to create the minimum window, with $*$'s used to denote the coupled method. Fig. 6 shows a sample task, with the two segmentation results overlaid on each other in gray. Coupled segmentation would select only the darker area for both anatomical and kinematic movement analysis.

Kinematic and anatomical joint measurements were directly compared. Then, two measures of movement smoothness were computed. Robotic exoskeletons are typically used to assess multi-DOF movements in the task space, with metrics such as the correlation ρ to a minimum jerk speed profile [10], and the spectral arc length [11]. These task-space metrics are computed on a movement's tangential velocity, which would reduce errors caused by joint misalignment. We used the MATLAB function and default settings from Balasubramanian et. al [11] to calculate the spectral arc length. Results were considered outliers if their value fell outside of 3 interquartile ranges past hinges [16]. All movements were analyzed together, since the goal of this analysis is not the preservation of any particular movement property dependent on movement speed or direction, but rather the comparison between anatomical and kinematic joint angle measurements.

III. EXPERIMENTAL RESULTS

The results of the pointing task experiment quantify the effects of estimating anatomical wrist joint angles with robot kinematic measurement, in the joint and task space.

A. Position Measurement Comparison

Kinematic and anatomical joint measurements were compared for all trajectories. We computed RMS errors between the two measurements, along with standard deviations (see Table I), treating the anatomical measurements obtained from motion capture as ground truth so that we could evaluate the accuracy of kinematic measurement of wrist orientation.

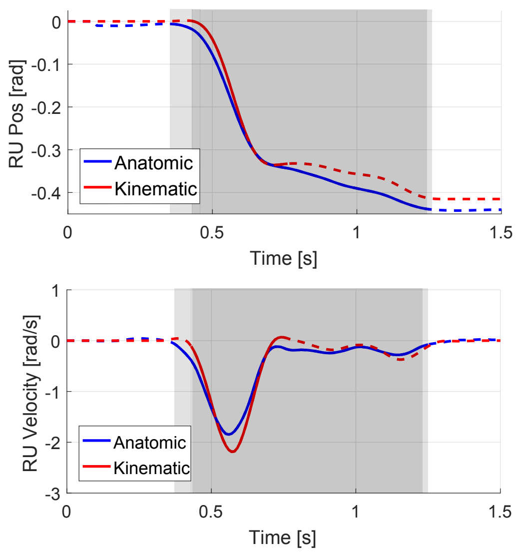

Fig. 6. RU trajectory taken from outbound movement. Segmentation is indicated via semi-transparent gray windows about the movement.

In general, human and robot joint axis misalignment drove the errors shown in Table I, which is separated by target and anatomical joint axis. The large error observed in Target 4 is partially attributable to range of motion limitations of the robotic mechanism. This particular ROM limitation is likely a result of the device being designed for ADL ranges, and not the arbitrary range imposed during our test, as well as the definition of neutral for the experiment being different than of the device's. While the errors for each target were small, the relatively large standard deviation of these values suggests that the intersubject variability of wrist axes direction detracts from the accuracy of using robot kinematics to infer measures in anatomical joint space.

B. Smoothness Measures

The movement smoothness metrics ρ (correlation to a minimum jerk velocity profile) and SAL (spectral arc length) were computed from the kinematic and anatomic joint motion measurements and are presented in Fig. 7a and 7b. These metrics were computing using segmentation based only on the observed measurements (i.e. segmentation of kinetic data is independent of segmentation of anatomic data).

In Fig. 7c and 7d, differences in smoothness metrics computed with kinematic and anatomic joint measurements are plotted for independent segmentation, and for segmentation based on the minimum movement time for the two data sets ($*$). Results suggest that ρ is highly sensitive to segmentation scheme, while SAL is not, as observed by the changes in the range of values in Fig. 7c and 7d.

TABLE I
RMS ERROR AND STANDARD DEVIATION (σ) BETWEEN KINEMATIC AND ANATOMICAL MEASUREMENTS

Target		Anatomical RU RMS [rad]	Anatomical RU σ [rad]	Anatomical FE RMS [rad]	Anatomical FE σ [rad]
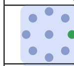	1	0.055	0.041	0.089	0.087
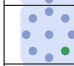	2	0.034	0.024	0.061	0.035
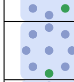	3	0.023	0.016	0.050	0.032
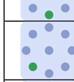	4	0.062	0.043	0.079	0.058
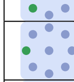	5	0.034	0.028	0.050	0.031
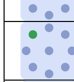	6	0.017	0.010	0.034	0.019
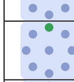	7	0.016	0.010	0.022	0.016
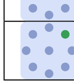	8	0.032	0.019	0.040	0.029

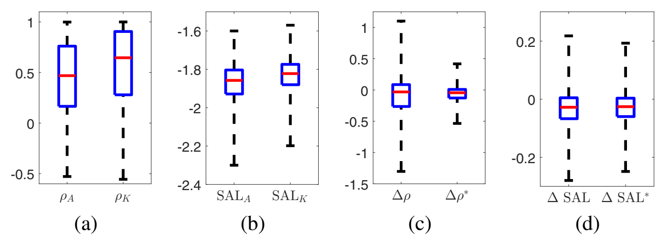

Fig. 7. Smoothness measures ρ and SAL, calculated from anatomic (A) and robot kinematic (K) measurements across all subjects, and all targets are shown in (a) and (b), respectively. For all plots, whiskers extend to three interquartile ranges past hinges. Qualitatively, (a) and (b) reflect the high variability of ρ and robustness of spectral arc length across measurement modalities found during the experiment. The difference between anatomic and kinematic ρ and SAL for each task, defined as $\Delta = Anatomic - Kinematic$ are shown in (c) and (d), respectively. The $*$ indicates the use of the minimum movement time for the two data sets.

IV. DISCUSSION

The goal of this work was to quantify the impact of joint misalignment and movement with respect to the robot on the relation between robot kinematic and human anatomic measurements. The sample pointing task in Fig. 6 displays a few of the characteristics we wished to investigate. Specifically, the combined effects of static friction driving the kinematic velocity to zero after the first velocity peak and inertia delaying and 'smoothing' on movement metrics were of interest. The trajectory shows both the effects of movement within the device, as well as errors arising from joint axis misalignment. In general, when comparing position measurements, the kinematic measurement fails to capture small variations in wrist movements relative to the device. Also, the imposition of orthogonal axes of rotation insufficiently captures actual anatomical motions. While our experiments involved only able-bodied participants, these issues are independent of population and remain relevant for the task of rehabilitation and assessment.

Researchers often present robotic rehabilitation outcomes in terms of measures based on movement velocity profiles, such as ρ (smoothness correlation) and spectral arc length, rather than reporting the trajectory data directly. Results in Fig. 7 show large variance in movement smoothness, which is not typical of healthy pointing movements. This variance could be attributed to the mapping created for the visualization, and perhaps required more training movements before subjects became comfortable with the mapping. Or, it is possible that wearing the exoskeleton device perturbed movements. Note that the correlation to a minimum jerk trajectory, ρ, is not consistent between joint encoder and motion capture data for this experiment and is sensitive to segmentation method. Looking at both Fig. 7b and 7d, the same trends discussed by Balasubramian et. al are apparent, namely, that spectral arc length is a more robust metric for quantifying smoothness, and is less sensitive than ρ to changes in segmentation. The smaller variance in SAL, both in magnitude and as a proportion of the expected value range supports the use of robotic kinematic data for this measure.

In general, any discussion of accuracy of joint-space anatomical measurements hinges on uncertainties in approximations made in the anatomical axes definitions. While imposing orthogonality on the direction of the average anatomical wrist axes, as described in Fig. 4, places some limitations on the accuracy of the model, it is both sufficiently accurate for the task, and appropriate for comparisons to robotic measurements of metrics which use tangential velocity, such as ρ and spectral arc length. Additionally, the inability of subjects to perform perpendicular wrist movements, even when guided by an exoskeleton is noteworthy. Angles between the anatomically determined axes for calibrations ranged from approximately 75° to 100°, similar to the results presented by Biryukova et. al [18]. This coupling of rotations suggests that analyses of movements about perpendicular flexion/extension and radial/ulnar deviation axes may obscure important coupled characteristics. Since the anatomic joint measurements were used for the task, most movements required multi-DOF robot movement, which could explain the wide range of smoothness scores, if friction and inertia impact smoothness.

To improve the qualitative observations about the data set shown in Fig. 7, we next examined the correlation between the anatomic and kinematic measurements, shown in Fig. 8. A high correlation suggests consistency across measurement modalities, indicating that kinematic data is an appropriate estimation of anatomic movements. First, there is a positive strong correlation between the smoothness metrics computed from kinematic data and those derived from 'ground truth' anatomic data, supporting the use of this exoskeleton as a measurement device. The quality of the correlations of ρ drastically improve once segmentation is coupled, rather than independent. This change is largely the result of independently segmented anatomic measurements capturing significantly more corrective and subtle motion at the end of the trajectories, as shown in Fig. 6, which are obscured by robotic joint static friction in kinematic measurements. Smoothness metrics computed from kinematic data are strongly correlated to anatomic data when the metrics are computed for identical segments of data, suggesting that care need be taken when designing segmentation algorithms for kinematic measure of human joint movements.

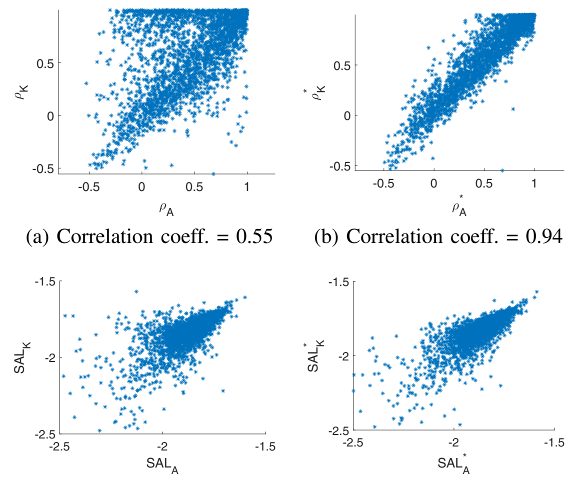

(a) Correlation coeff. = 0.55 (b) Correlation coeff. = 0.94

(c) Correlation coeff. = 0.57 (d) Correlation coeff. = 0.76

Fig. 8. Anatomical vs. kinematic metrics calculations of ρ (a,b) and SAL (c,d) for both independent (a,c) and coupled (b,d) segmentation strategies. High correlation coefficients indicate that kinematic measurement accurately captures anatomical movements.

In Fig. 9, we present correlations between independent and coupled segmentation methods applied in the calculation of smoothness metrics derived from a single data source (anatomical or kinematic). For both measures, there is a high correlation between the kinematic measures calculated using the independent and coupled segmentation algorithm, indicating that kinematic data is robust to changes in segmentation strategy. This correlation is expected since the robotic device's inertia and friction delay the start and hasten the end of trajectories. The correlations of measures calculated from anatomical trajectories were lower, due to the capture of more movements with respect to the robot. However, the higher correlation for SAL across segmentation strategies further supports it as robust to changes in segmentation and measurement modalities. Looking at Fig. 9 it is clear that the change in segmentation strategy has less of an effect on SAL overall than it did for ρ.

The 'improvement' in scores based on segmentation method supports the idea that the robot kinematic measures capture the bulk movement properly, that is to say, velocity segmentation on the anatomical trajectories did not typically remove as many submovements, corrections, or tremors, as the robot did, which is to be expected for a device with low, but still non-negligble inertia and static friction. For analyses on gross, segmented movements, our results demonstrate that robot kinematic measurement accurately captures human movement characteristics.

V. CONCLUSIONS

Robots employed for rehabilitation applications are often used as assessment tools. It is typically assumed that the joint axes of an exoskeleton are aligned with the joint axes of the individual, allowing assessment of movement coordination

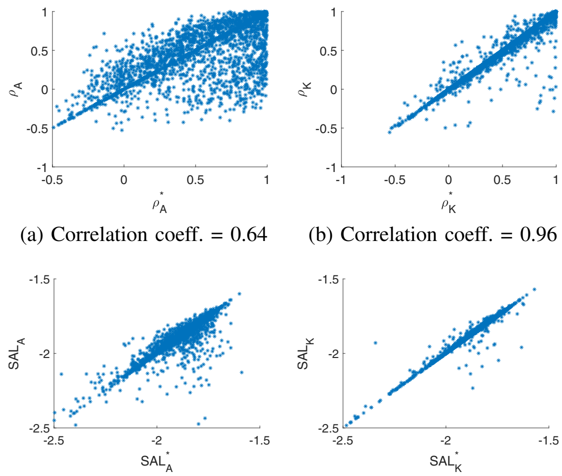

(a) Correlation coeff. = 0.64 (b) Correlation coeff. = 0.96

(c) Correlation coeff. = 0.78 (d) Correlation coeff. = 0.97

Fig. 9. Effect of segmentation on each of the metrics, as calculated from anatomical data (a,c) and kinematic data (b,d). On all vertical axes, the metrics are calculated with individual segmentation, and the horizontal axes are the metrics calculated with coupled segmentation. The higher correlation coefficients for kinematic measures indicate that robotic measurement is less sensitive to segmentation strategies.

in both joint space and task space. For multi-articular joints such as the wrist, this assumption can break down. In this paper, we evaluated the accuracy of anatomical joint axis measurement using the encoders of a wrist exoskeleton robot module compared to ground truth measurements of anatomical movements from a motion capture system. We found that, as expected, the kinematic robot measures failed to capture movements of the wrist relative to the robot. While these errors manifest in any trajectory-based metrics, for movement quality metrics, the measurements from robot sensor data are more reliable. Two measures of movement smoothness derived from task space velocity profiles were evaluated for a target hitting task performed by able bodied subjects. For performance measure ρ, that characterizes the correlation between the subjects task space velocity profile and an optimally smooth profile, we found that segmentation differences in kinematic data versus anatomical data accounted for the variations. If a coupled segmentation method was used, restricting the data set to span the same time period regardless of data used for metric computation, the kinematic and anatomical data produced strongly correlated metrics. Spectral arc length, which measures movement smoothness in the frequency domain, was less dependent on segmentation method, and SAL computed with kinematic data was strongly correlated to SAL computed with anatomical joint motion data. We conclude that the data from a robotic wrist exoskeleton can be reliably used to compute movement smoothness metrics for target hitting tasks, even though such measurements fail to capture relative motion of the wrist compared to the exoskeleton device.

Acknowledgments

The authors would like to acknowledge Evan Pezent as the designer of the OpenWrist and Fabrizio Sergi for advice in the development of the experimental methods and anatomical wrist model. This work was supported by NSF-CPS-1135949/1135916 and NSTRF-NNX13AM70H.

References

[1] P. S. Lum *et al.*, "Robotic approaches for rehabilitation of hand function after stroke," *American J. of Physical Medicine & Rehabilitation*, vol. 91, no. 11, pp. S242–S254, 2012.
[2] P. Maciejasz *et al.*, "A survey on robotic devices for upper limb rehabilitation," *J. of Neuroengineering and Rehabilitation*, vol. 11, no. 1, p. 3, 2014.
[3] A. A. Blank *et al.*, "Current trends in robot-assisted upper-limb stroke rehabilitation: promoting patient engagement in therapy," *Current Physical Medicine and Rehabilitation Reports*, vol. 2, no. 3, pp. 184–195, 2014.
[4] A. U. Pehlivan, *et al.*, "Design and validation of the ricewrist-s exoskeleton for robotic rehabilitation after incomplete spinal cord injury," *Robotica*, vol. 32, no. 08, pp. 1415–1431, 2014.
[5] L. Masia *et al.*, "Performance adaptive training control strategy for recovering wrist movements in stroke patients: a preliminary, feasibility study," *J. of NeuroEngineering and Rehabilitation*, vol. 6, no. 1, p. 44, 2009.
[6] C. G. Rose, *et al.*, "Characterization of a hand-wrist exoskeleton, readapt, via kinematic analysis of redundant pointing tasks," in *Rehabilitation Robotics (ICORR), IEEE Intl. Conf. on*, 2015, pp. 205–210.
[7] S. Kalsi-Ryan *et al.*, "Development of the graded redefined assessment of strength, sensibility and prehension GRASSP: reviewing measurement specific to the upper limb in tetraplegia," *J. of Neurosurgery: Spine*, vol. 17, pp. 65–76, 2012.
[8] V. Mathiowetz *et al.*, "Adult norms for the box and block test of manual dexterity," *American J. of Occupational Therapy*, vol. 39, no. 6, pp. 386–391, 1985.
[9] K. Tyryshkin *et al.*, "A robotic object hitting task to quantify sensorimotor impairments in participants with stroke," *J. of Neuroengineering and Rehabilitation*, vol. 11, no. 1, p. 47, 2014.
[10] O. Celik *et al.*, "Normalized movement quality measures for therapeutic robots strongly correlate with clinical motor impairment measures," *IEEE Trans. on Neural Systems and Rehabilitation Engineering*, vol. 18, no. 4, pp. 433–444, 2010.
[11] S. Balasubramanian *et al.*, "A robust and sensitive metric for quantifying movement smoothness," *IEEE Trans. on Biomedical Engineering*, vol. 59, no. 8, pp. 2126–2136, 2012.
[12] E. Pezent *et al.*, "Design and characterization of the openwrist: A robotic wrist exoskeleton for coordinated hand-wrist rehabilitation," in *Rehabilitation Robotics (ICORR), IEEE Intl. Conf. on*, 2017.
[13] P. Agarwal *et al.*, "Design, control and testing of a thumb exoskeleton with series elastic actuation," *Intl. J. of Robotics Research*, 2017.
[14] M. Esmaeili, *et al.*, "Hyperstaticity for ergonomie design of a wrist exoskeleton," in *Rehabilitation Robotics (ICORR), IEEE Intl. Conf. on*, 2013, pp. 1–6.
[15] S. K. Charles and N. Hogan, "The curvature and variability of wrist and arm movements," *Experimental Brain Research*, vol. 203, no. 1, pp. 63–73, 2010.
[16] K. D. Fitle, *et al.*, "A robotic exoskeleton for rehabilitation and assessment of the upper limb following incomplete spinal cord injury," in *Robotics and Automation (ICRA), IEEE Intl. Conf. on*, 2015, pp. 4960–4966.
[17] J. J. Crisco *et al.*, "The mechanical axes of the wrist are oriented obliquely to the anatomical axes," *The J. of Bone & Joint Surgery*, vol. 93, no. 2, pp. 169–177, 2011.
[18] E. Biryukova *et al.*, "Kinematics of human arm reconstructed from spatial tracking system recordings," *J. of Biomechanics*, vol. 33, no. 8, pp. 985 – 995, 2000.
[19] R. Schmidt *et al.*, "A marker-based measurement procedure for unconstrained wrist and elbow motions," *J. of Biomechanics*, vol. 32, no. 6, pp. 615–621, 1999.
[20] A. Savitzky and M. J. Golay, "Smoothing and differentiation of data by simplified least squares procedures." *Analytical Chemistry*, vol. 36, no. 8, pp. 1627–1639, 1964.
[21] B. Rohrer, S. Fasoli, H. I. Krebs, R. Hughes, B. Volpe, W. R. Frontera, J. Stein, and N. Hogan, "Movement smoothness changes during stroke recovery," *J. of Neuroscience*, vol. 22, no. 18, pp. 8297–8304, 2002.
[22] H. I. Krebs, N. Hogan, M. L. Aisen, and B. T. Volpe, "Robot-aided neurorehabilitation," *IEEE Trans on Rehabilitation Engineering*, vol. 6, no. 1, pp. 75–87, 1998.